PHYSICAL REVIEW E **84**, 015203(R) (2011)

Stability of ring patterns arising from two-dimensional particle interactions

Theodore Kolokolnikov,[1] Hui Sun,[2] David Uminsky,[2] and Andrea L. Bertozzi[2]
[1]*Department of Mathematics and Statistics, Dalhousie University, Halifax, Canada*
[2]*Department of Mathematics, UCLA, Los Angeles, California 90095, USA*
(Received 11 May 2011; published 22 July 2011)

Pairwise particle interactions arise in diverse physical systems ranging from insect swarms to self-assembly of nanoparticles. In the presence of long-range attraction and short-range repulsion, such systems can exhibit bound states. We use linear stability analysis of a ring equilibrium to classify the morphology of patterns in two dimensions. Conditions are identified that assure the well-posedness of the ring. In addition, weakly nonlinear theory and numerical simulations demonstrate how a ring can bifurcate to more complex equilibria including triangular shapes, annuli, and spot patterns with N-fold symmetry. Many of these patterns have been observed in nature, although a general theory has been lacking, in particular how small changes to the interaction potential can lead to large changes in the self-organized state.

DOI: 10.1103/PhysRevE.84.015203 PACS number(s): 89.75.Kd, 05.45.−a

Collective behavior of interacting systems [1] is a captivating natural phenomenon. Such systems form patterns that inspire evolutionary [2] and biological [3] questions as well as structural and physical ones. More recently, such natural behavior has inspired intelligent design of control algorithms for unmanned vehicles. Particle interaction models are extremely prevalent in the biology literature in many contexts such as insect aggregation [4] and locust swarms [5]; however they also arise in other important physics applications such as self-assembly of nanoparticles [6], theory of granular gases [7], and molecular dynamics simulations of matter [8]. Regardless of whether the model is meant to describe a complex biological system such as a flock, a bacterial colony, or a locust swarm, or a basic physics application derived from first principles, a common feature of all particle interaction models is the attractive-repulsive nature of the potential. Often a "steady state" pattern can be formulated as a minimizer of a pairwise interaction energy

$$E(\vec{x}) = \sum_{i,j\neq i} P(|x_i - x_j|) \tag{1}$$

for some potential P.

Typically, $P(r)$ is a convex function having a single positive minimum, $\vec{x}$ is the position vector of N particles. A potential $P(r)$ is called *confining* if the diameter $d = \max_{i,j} |x_i - x_j|$ of the steady state is bounded as $N \to \infty$. For confining potentials, the equilibrium configuration is a minimizer of a high dimensional nonconvex problem for which a fully developed predictive theory is elusive. Our analysis specifically applies to such potentials.

Recent analysis [9] shows that scaling behavior of equilibrium configuration depends on the classical H-stability properties of the interaction potential [10] but does not provide a theory for symmetry breaking of the equilibrium configuration. The last five years has seen a surge of interest in the physics literature for confining potentials which tend to yield complex equilibrium patterns. One particularly interesting question is how to infer properties of the local interactions from large scale behavior of the self-organized state [11]. On the other hand, self-assembly in materials involves design of interaction potentials that lead to desired complex structures [12].

The goal of this letter is to develop a theory for prediction and classification of equilibrium patterns based on properties of the interaction potential. For simplicity, we present case studies from two different families of interaction forces $F(r) = -P'(r)$, the power law force

$$F(r) = r^p - r^q; \quad 0 \leqslant p < q \tag{2}$$

and a smoothed step discontinuity

$$F(r) = \tanh[(1-r)a] + b; \; 0 < a; \; -\tanh(a) < b < 1. \tag{3}$$

Both of these families yield confined patterns, so that the spatial extent of the pattern remains bounded as $N \to \infty$. Minimizers of (1) with confining potentials can exhibit intricate structure as shown in Fig. 1 for case (3). Note the complex patterns ranging from rings and annuli to more complex structures exhibiting period two and three symmetry breaking to very complex "soccer ball" like shapes. Related patterns (in particular the annuli and spotted patterns) have been observed in experiments of stressed bacterial colonies [13] which have associated related nonlocal models [14]. We present a methodology for analyzing structures of these patterns from basic properties of the interaction potential.

Our analysis is based on stability of the interaction energy under a gradient flow, although the results could be applied to more sophisticated interaction models such as those arising from the Morse potential considered in [9]. The gradient flow equations arising from (1) are

$$\frac{dx_j}{dt} = \frac{1}{N}\sum_{k,k\neq j} F(|x_j - x_k|)\frac{x_j - x_k}{|x_j - x_k|}, \quad j = 1,\ldots,N. \tag{4}$$

Simulation of this system with a large number of particles results in a long time equilibrium shape. The shapes in Fig. 1 are the result of a forward Euler time integration of (4) with $N = 5000$, computed to $t = 1000$ with $dt = 0.5$. Up to rotation, the results are independent of initial condition, typically taken to be randomly distributed inside a unit square. A well-known approach in pattern formation is to consider stability of a constant state for which theory can often be derived in analytic form, and then consider bifurcations from that state to understand structures of patterns. Since the potential is confining, it does not make sense to consider

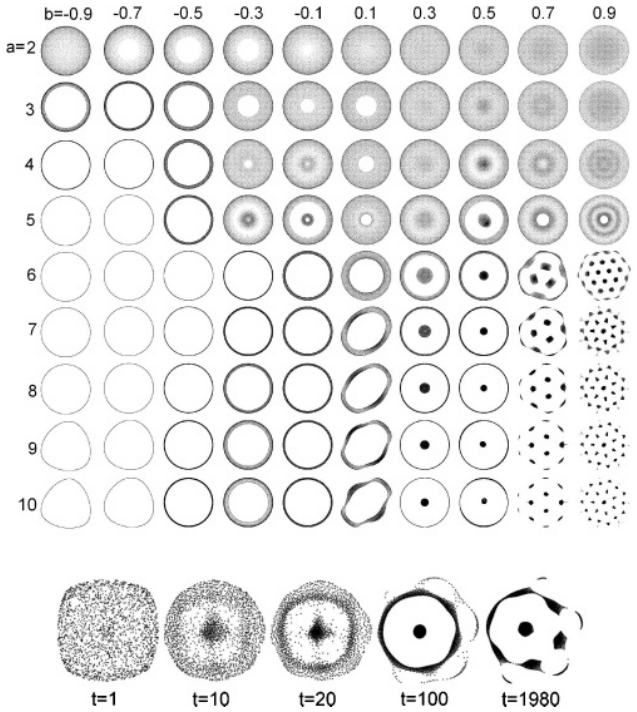

FIG. 1. Top: Minimizers of the energy (1) with force law (3). Diameter $d = \max_{i,j} |x_i - x_j|$ ranges from 0.3 in top left to 3 in bottom right. Bottom: time evolution of (4) with values $a = 8$, $b = 0.67$.

stability of "flat" states but rather that of "ring" states in which particles are concentrated at a particular radius, as seen, for example, in the lower left corner of Fig. 1. Any potential that has repulsion dominant in the near field and attraction dominant in the far field has an exact ring solution whose radius r_0 satisfies

$$\int_0^{\frac{\pi}{2}} F(2r_0 \sin\theta) \sin\theta d\theta = 0, \tag{5}$$

where we assume a continuum limit for N is large.

The ring is a special case of an extremum of (1) in which the particles concentrate on a one dimensional curve. In the limit $N \to \infty$ such curves satisfy the continuum equation [15]

$$\frac{\partial}{\partial t}\left(\rho \left|\frac{\partial z}{\partial \alpha}\right|\right) = 0, \quad \frac{\partial z}{\partial t} = K * \rho, \tag{6}$$

where $z(\alpha;t)$ is a parametrization of the curve, $\rho(\alpha;t)$ is its particle density, and $K * \rho = \int F(|z(\alpha) - z(\alpha')|)\frac{z(\alpha)-z(\alpha')}{|z(\alpha)-z(\alpha')|}\rho(\alpha',t)dS(\alpha')$ with dS denoting the arclength element. Formula (6) follows from conservation of mass and is a generalization of the classical Birkhoff-Rott equation for 2D vortex sheets [16] applied to gradient vector fields rather than divergence free flow. See Ref. [15] for details. Linear analysis of the B-R equation describes the classical Kelvin-Helmoltz instability in fluid dynamics and we use this as an analogy to our study of equilibrium patterns for the pairwise interaction energy (1).

Consider the perturbations of the ring of N particles of the form $x_k = r_0 \exp(2\pi i k/N)[1 + \exp(t\lambda)\phi_k]$, where $\phi_k \ll 1$. After some algebra we obtain

$$\lambda\phi_j = \frac{1}{N}\sum_{\substack{k=1..N \\ k\neq j}} G_+\left(\frac{\pi(k-j)}{N}\right)\left[\phi_j - \phi_k \exp\left(\frac{2\pi i(k-j)}{N}\right)\right]$$
$$+ G_-\left(\frac{\pi(k-j)}{N}\right)\left[\bar{\phi}_k - \bar{\phi}_j \exp\left(\frac{2\pi i(k-j)}{N}\right)\right],$$

where $j = 1,\ldots,N$, $G_\pm(\theta) = \frac{1}{2}(G_1 \pm G_2)$, and

$$G_1(\theta) = F'(2r_0|\sin\theta|), \quad G_2(\theta) = \frac{F(2r_0|\sin\theta|)}{2r_0|\sin\theta|}.$$

Next we substitute $\phi_j = b_+ e^{2m\pi ij/N} + b_- e^{-2m\pi ij/N}$ where we assume that $b_\pm$ are real, and m is a strictly positive integer. This leads to a 2×2 eigenvalue problem $\lambda\binom{b_+}{b_-} = M(m)\binom{b_+}{b_-}$, where

$$M(m) := \begin{bmatrix} I_1(m) & I_2(m) \\ I_2(m) & I_1(-m) \end{bmatrix}, \quad m = 1,2,\ldots, \tag{7}$$

$$I_1(m) = \frac{4}{N}\sum_{l=1}^{N/2} G_+\left(\frac{\pi l}{N}\right)\sin^2\left[(m+1)\frac{\pi l}{N}\right],$$

$$I_2(m) = \frac{4}{N}\sum_{l=1}^{N/2} G_-\left(\frac{\pi l}{N}\right)\left[\sin^2\left(\frac{\pi l}{N}\right) - \sin^2\left(m\frac{\pi l}{N}\right)\right].$$

Taking the limit $N \to \infty$, we obtain

$$I_1(m) = \frac{4}{\pi}\int_0^{\frac{\pi}{2}} G_+(\theta)\sin^2[(m+1)\theta]\,d\theta, \tag{8a}$$

$$I_2(m) = \frac{4}{\pi}\int_0^{\frac{\pi}{2}} G_-(\theta)[\sin^2(\theta) - \sin^2(m\theta)]d\theta. \tag{8b}$$

The ring is linearly stable if the eigenvalues λ of (7) are nonpositive for all integers $m \geqslant 1$; otherwise it is unstable. There are two possible types of instabilities. Ones in which the ring is *long-wave unstable*, corresponding to an instability of a low order mode (small m) but stability of higher order modes. The second type corresponds to ill-posedness of the ring in which the eigenvalues are positive in the $m \to \infty$ limit and grow as m increases. In the latter case the ring completely breaks up and often forms a fully two-dimensional pattern. Ill-posedness in curve evolution problems is known in other problems, most notably the Kelvin-Helmholtz instability of the 2D vortex sheet [15,16]. However the types of nonlinear structures seen here are completely different from the vortex roll-up behavior familiar from incompressible fluids.

An example of a stable ring is provided by the force $F(r) = r - r^2$, for which the matrix $M(m)$ and its eigenvalues can be explicitly computed. More generally, if $F(0) > 0$ and F is C^2, the asymptotics for large m yield trace $M(m) \sim \frac{F(0)}{\pi r_0}\ln m > 0$ as $m \to \infty$, so that all high modes m are unstable. It follows that a necessary condition for well-posedness of a ring is that

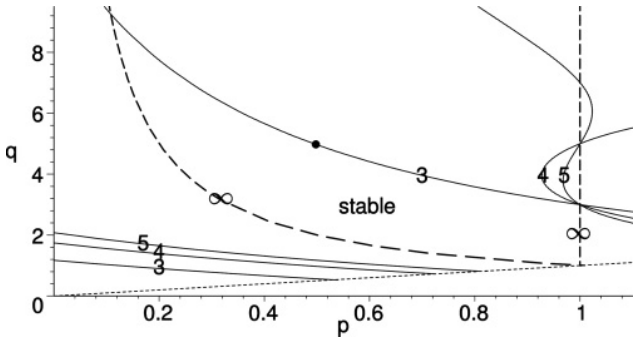

FIG. 2. Stability region for (2). The curves shown correspond to the boundaries of the stability $\det[M(m)] = 0$, with $m = 3, 4, 5$ and $m = \infty$, as indicated. The line $p = q$ is also drawn. Crossing any of the curves destabilizes the ring. The intersection of $m = \infty$ and $m = 3$ boundaries is at $p = 0.10779$, $q = 9.277102$. Black dot is the position where we compute the pitchfork bifurcation in Fig. 3.

$F(0) = 0$. If in addition, F is C^4, then using integration by parts we obtain

$$\text{tr } M(m) \sim \frac{2}{\pi}\int_0^{\pi/2}\left[\frac{F(2r_0\sin\theta)}{2r_0\sin\theta} - F'(2r_0\sin\theta)\right]d\theta + O\left(\frac{1}{m^2}\right),$$

$$\det[M(m)] \sim \text{tr } M(m)\frac{F''(0)r_0}{m^2} + O\left(\frac{1}{m^4}\right).$$

In summary, if $F(r)$ is C^4 on $[0,2r_0]$, then sufficient conditions for linear well-posedness of a ring are

$$F(0) = 0,\ F''(0) < 0, \quad \int_0^{\pi/2} G_1(\theta) + G_2(\theta)d\theta < 0. \quad (9)$$

In particular, the ring solution for the force (3) is always ill-posed, since $F(0) > 0$. Another general result is if F is odd and C^∞ on $[0,2r_0]$, where $\det[M(m)] = 0$ for all m; the ring then has infinitely many zero eigenvalues. This observation may be relevant for the Kuramoto model $F(r) = \sin(r)$ [17].

For the force of type (2) with $0 < p < q$, the asymptotics of the mode $m = \infty$ can be computed in terms of γ functions. It is shown in [18] that the mode $m = \infty$ is stable if and only if $pq > 1$ and $p < 1$. In addition, the low modes $m = 2, 3, 4, \ldots$ may also become unstable (see Fig. 2). The dominant unstable mode corresponds to $m = 3$, which bounds the stability region from above. An implicit formula for the boundary can be computed analytically and it is shown in Fig. 2. Similarly, the stability boundary for $m = 2$ mode happens to lie well outside the area shown in Fig. 2. The stability boundaries for modes $m = 4, 5, \ldots$ are also expressed in terms of higher order polynomials in p,q.

We now use weakly nonlinear theory to analyze how the transition of stability occurs. Figure 3 is a bifurcation diagram for interaction force (2), taking $p = 0.5$, where we record the change of the quantity $\Delta r = r_M - r_m$ according to the bifurcation parameter q, with r_M and r_m being the maximum and minimum of the displacement from the origin. Numerical simulation for the whole system (4) are done with 100 particles with random initial condition, plotted as black dots. At $q = 4.95$ the steady state solution remains a stable ring; while at

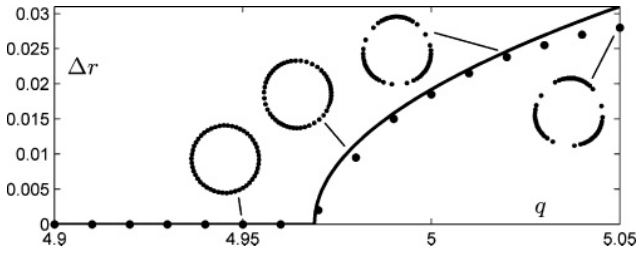

FIG. 3. Bifurcation diagram for interaction force (2), with $p = 0.5$. The solid curve is derived from weakly nonlinear analysis; while the dots are simulations of (4).

$q = 4.98$ the 3 mode becomes slightly unstable and the points tend to move tangentially to break the ring into a triangular shape. By further increasing q, the points on the curve continue to move toward a more triangular shape. The weakly nonlinear analysis confirms that this process is in fact a supercritical pitchfork bifurcation. The analytical form of the pitchfork is given by as $\Delta r = \sqrt{\max[0,\tau(q - q_c)]}$, with $q_c \approx 4.9696$ and bifurcation value $\tau \approx 0.01188$, which is plotted as a solid line in Fig. 3. See Ref. [18] for detailed derivation.

In fact, a more general result can be stated as follows [18]: Near the stability transition of a fixed long-wave (small m) mode, if the interaction force has a nonvanishing first derivative with respect to the bifurcation parameter, a pitchfork bifurcation is always exhibited. For example, a mode three bifurcation occurs in the first column of Fig. 1 at the value $a \approx 7.912$, and second column at $a \approx 8.2115$.

Even if (4) is ill-posed in the *continuous* limit $N \to \infty$, the ring of *discrete* particles (4) may be stable with a relatively large N as in Fig. 4. Note the slight instability for $N = 160$ but stability when $N = 120$. The continuous limit is well approximated with $N = 5000$; the resulting steady state

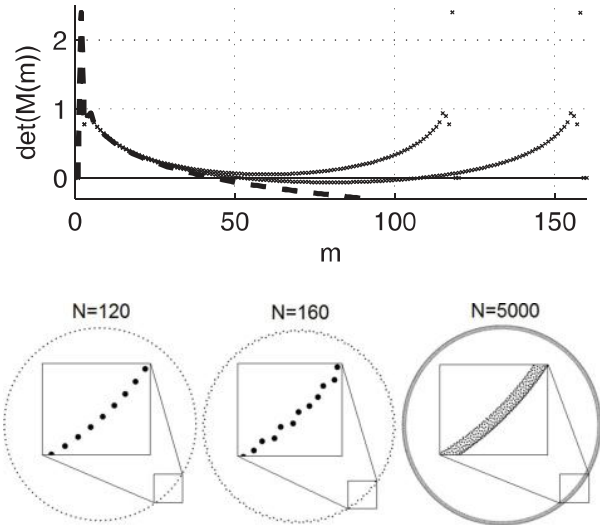

FIG. 4. Stability of discrete vs continuous system for $F(r) = \tanh[4(1 - r)] - 0.5$. Top: $\det[M(m)]$. Dashed line corresponds to continuum Eq. (10) and crosses to discrete Eq. (9) with $N = 120, 160$. Instability occurs iff $\det[M(m)] < 0$. Bottom: steady states of discrete dynamics with N as indicated; inserts show the blowup of the ring structure.

appears to be a thin annulus, whose inner and outer radius are approximately r_0 given by (5). See Ref. [18] for detailed analysis.

So far we have concentrated on simple forces (2), (3) which do not decay for large r. However this is not a crucial restriction. For example, take $F(r) = (r - r^2)\exp(-ar)$. It can be shown that a ring solution exists for all $0 \leqslant a \leqslant 3.245$ and is stable for all $0 \leqslant a \leqslant 0.923$. As a is increased past 0.923, the ring becomes ill-posed due to the violation of the third equation in (9). In general, one can add sufficient far-field decay without changing our analysis.

Numerics suggest that random initial conditions tend to converge to ring solutions, whenever the ring is stable. Global stability of the ring remains an open question.

T.K. is supported by NSERC Grant 47050. D.U. is supported by NSF Grant DMS-0902792 and supported by UC Presidents Fellowship program. A.B. and H.S. are supported by NSF Grants DMS-0907931 and EFRI-1024765 and ONR Grant N000141010641. We thank the anonymous referees for their careful reading and useful suggestions. We thank Andrew Bernoff for helpful comments.

[1] S. Camazine *et al.*, *Self Organization in Biological Systems* (Princeton University Press, Princeton, 2003); I. Prigogine, *Order Out of Chaos* (Bantam, New York, 1984).

[2] J. K. Parrish and L. Edelstein-Keshet, Science **284**, 99 (1999); S. A. Kaufmann, *The Origins of Order: Self-Organization and Selection in Evolution* (Oxford University Press, New York, 1933).

[3] I. D. Couzin, J. Krauss, N. R. Franks, and S. A. Levin, Nature (London) **433**, 513 (2005); I. Reidel, K. Kruse, and J. Howard, Science **309**, 300 (2005); G. Flierl, D. Grünbaum, S. A. Levin, and D. Olson, J. Theor. Biol. **196**, 397 (1999).

[4] A. Mogilner, L. Edelstein-Keshet, L. Bent, and A. Spiros, J. Math. Biol. **47**, 353 (2003); L. Edelstein-Keshet, J. Watmough, and D. Grunbaum, *ibid.* **36**, 515 (1998).

[5] C. M. Topaz, A. J. Bernoff, S. Logan, and W. Toolson, Eur. Phys. J. Special Topics **157**, 93 (2008); C. M. Topaz, A. L. Bertozzi, and M. A. Lewis, Bull. Math. Biol. **68**, 1601 (2006); A. J. Leverentz, C. M. Topaz, and A. J. Bernoff, SIAM J. Appl. Dyn. Sys. **8**, 880 (2009).

[6] D. D. Holm and V. Putkaradze, Phys. Rev. Lett. **95**, 226106 (2005).

[7] N. V. Brilliantov and T. Pöschel, in *Granular Gases*, Lecture Notes in Physics, Vol. 564, (Springer, Berlin, 2000); R. Ramirez, T. Pöschel, N. V. Brlliantov, and T. Schwager, Phys. Rev. E **60**, 4465 (1999); G. Toscani, RAIRO Modél Math. Anal. Numer. **34**, 1277 (2000).

[8] J. M. Haile, *Molecular Dynamics Simulation: Elementary Methods* (John Wiley and Sons, New York, 1992).

[9] H. Levine, W. J. Rappel, and I. Cohen, Phys. Rev. E **63**, 017101 (2000); M. R. D'Orsogna, Y. L. Chuang, A. L. Bertozzi, and L. S. Chayes, Phys. Rev. Lett. **96**, 104302 (2006); Y.-L. Chuang, M. R. D'Orsogna, D. Marthaler, A. L. Bertozzi, and L. Chayes, Physica D **232**, 33 (2007).

[10] D. Ruelle, *Statistical Mechanics* (Benjamin, New York, 1969).

[11] R. Lukeman, Y.-X. Li, and L. Edelstein-Keshet, PNAS **107**, 12576 (2010).

[12] M. C. Rechtsman, F. H. Stillinger, and S. Torquato, Phys. Rev. Lett. **95**, 228301 (2005); Phys. Rev. E **75**, 031403 (2007); H. Cohn and A. Kumar, PNAS **106**, 9570 (2009).

[13] L. Tsimring, H. Levine, I. Aranson, E. Ben-Jacob, I. Cohen, O. Shochet, and W. N. Reynolds, Phys. Rev. Lett. **75**, 1859 (1995); A. M. Delprato, A. Samadani, A. Kudrolli, and L. S. Tsimring, *ibid.* **87**, 158102 (2001).

[14] E. F. Keller and L. A. Segel, J. Theor. Biol. **30**, 225 (1971); M. P. Brenner, P. Constantin, L. P. Kadanoff, A. Shenkel, and S. C. Venkataramani, Nonlinearity **12**, 1071 (1999; M. P. Brenner, L. S. Levitov, and E. O. Budrene, Biophys. J. **74**, 1677 (1998).

[15] H. Sun, D. Uminsky, and A. Bertozzi, SIAM J. Appl. Math. (submitted).

[16] R. Krasny, J. Fluid Mech. **167**, 65 (1986).

[17] S. H. Strogatz, Physica D **143**, 1 (2000).

[18] H. Sun, T. Kolokolnikov, D. Uminsky, and A. Bertozzi, preprint 2011.